SENCKENBERG

ORIGINAL PAPER

Digging deep: lessons learned from meiofaunal responses to a disturbance experiment in the Clarion-Clipperton Zone

Nene Lefaible[1] · Lara Macheriotou[1] · Kaveh Purkiani[2,3] · Matthias Haeckel[2] · Daniela Zeppilli[4] · Ellen Pape[1] · Ann Vanreusel[1]

Abstract

The deep-sea mining industry is currently at a point where large-sale, commercial polymetallic nodule exploitation is becoming a more realistic scenario. At the same time, certain aspects such as the spatiotemporal scale of impacts, sediment plume dispersion and the disturbance-related biological responses remain highly uncertain. In this paper, findings from a small-scale seabed disturbance experiment in the German contract area (Clarion-Clipperton Zone, CCZ) are described, with a focus on the soft-sediment ecosystem component. Despite the limited spatial scale of the induced disturbance on the seafloor, this experiment allowed us to evaluate how short-term (< 1 month) soft-sediment changes can be assessed based on sediment characteristics (grain size, nutrients and pigments) and metazoan meiofaunal communities (morphological and metabarcoding analyses). Furthermore, we show how benthic measurements can be combined with numerical modelling of sediment transport to enhance our understanding of meiofaunal responses to increased sedimentation levels. The lessons learned within this study highlight the major issues of current deep-sea mining-related ecological research such as deficient baseline knowledge, unrepresentative impact intensity of mining simulations and challenges associated with sampling trade-offs (e.g., replication).

Keywords Deep-sea mining · Polymetallic nodules · Meiofauna · Impact studies · Sediment plume · Numerical modelling

Introduction

The abyssal seafloor (4–5 km depth) of the Clarion-Clipperton Zone (CCZ) represents the largest known deposit of polymetallic nodules on Earth (ISA 2011). They are composed of commercially important metals (e.g., cobalt, nickel and copper), which has led to a strong interest from the mining industry to extract these mineral concretions (Miller et al. 2018). The development of technologies to mine the mineral resources at the deep-seabed has progressed rapidly in recent years and so far two contractors have tested prototype mining vehicles in their license areas in the CCZ (2021: GSR, https://www.deme-group.com and 2022: NORI, https://metals.co/nori/). As more follow-up trials are planned, it can be stated that this emerging industry is at a tipping-point in its development where large-scale mining is becoming a realistic scenario (Miller et al. 2018). Whereas different mining techniques are possible, most of the proposed operations are based on a similar concept: minerals will be harvested by a collector vehicle, transported vertically by a lifting system through the water column where a surface water support vessel will be used for ore cleaning and transport to land (Levin et al. 2016; Miller et al. 2018; Christiansen et al. 2020). It is expected that all three units of the seabed mining operational system (i.e., collector vehicle, riser pipes and surface vessel) will exert significant environmental pressures on several ecosystem components, directly and indirectly throughout the sediment–water interface and the water

✉ Nene Lefaible
Nene.Lefaible@UGent.be

1 Marine Biology Research Group, Ghent, Belgium

2 GEOMAR Helmholtz Centre for Ocean Research Kiel, Kiel, Germany

3 MARUM Centre for Marine Environmental Sciences and Faculty of Geosciences, University of Bremen, Bremen, Germany

4 University Brest, CNRS, Ifremer, UMR6197 Biologie Et Ecologie Des Ecosystèmes Marins Profonds, 29280 Plouzané, France

column (Thiel et al. 2001; Christiansen et al. 2020; Amon et al. 2022). Therefore, robust environmental impact assessment (EIA) strategies are indispensable to correctly identify and quantify potential impacts, along with the formulation of clear environmental management objectives (Foley et al. 2015; Boetius and Haeckel 2018; Durden et al. 2018).

Not only the polymetallic nodule-associated fauna, but also the soft-sediment assemblages are thought to be sensitive to these activities (Thiel et al. 2001; Vanreusel et al. 2016; Washburn et al. 2019; Christiansen et al. 2020). Meiofauna and more specifically, nematodes, represent the most abundant and diverse constituents of deep-sea metazoan benthos and are mainly concentrated within the upper sediment layers (0–10 cm) (Miljutin et al. 2011; Pape et al. 2017, 2021; Hauquier et al. 2019; Lins et al. 2021; Tong et al. 2022). Therefore, the removal and reworking (suspension and re-deposition) of the upper sediment layers during nodule collection and potential faunal mortality and dislocation, together with indirect effects such as sediment plume dispersal, will affect the distribution and recovery of these organisms (Miljutin et al. 2011; Gollner et al. 2017; Smith et al. 2020). Multiple small-scale disturbance experiments have already been performed within the CCZ (reviewed by Jones et al. 2017). Despite their methodological differences (e.g., sampling location, disturbance device and temporal resolution), all experiments induced direct physical seabed alterations and some level of sediment resuspension (Jones et al. 2017 and references therein). The majority of the studies showed negative impacts on the soft-sediment meiofauna such as reduced densities and diversity one year after disturbance (Jones et al. 2017). Meiofaunal communities also showed signs of recovery in terms of density over time for some experiments (Jones et al. 2017), but a study by Miljutin et al. (2011) still found significantly lower nematode standing stock, diversity and a divergent community composition in a 30 year old disturbance track.

Even though these benthic impact experiments have led to important insights and contributed greatly to the description of mining-related pressures, they still represent simulated, scaled-down disturbances. Consequently, many of the proposed impacts and especially their spatial and temporal extent still remain poorly understood (Levin et al. 2016; Gollner et al. 2017; Jones et al. 2017; Christiansen et al. 2020). An additional uncertainty is the severity of indirect impacts such as those associated with the sediment plume discharge that is generated during nodule mining (Levin et al. 2016; Gollner et al. 2017; Jones et al. 2017; Christiansen et al. 2020). Studies on sediment plume dispersal are scarce with estimates of plume propagation varying from short ranges (10 s of km's) up to much wider ranges (100 s of km's), which leads to considerable uncertainty regarding the effective size of the impacted area after a mining disturbance

(Jones et al. 2017; Peukert et al. 2018; Muñoz-Royo et al. 2021; Purkiani et al. 2021; Weaver et al. 2022). It is however expected that the extent of this impact will depend on the design of the nodule collector vehicle and the amount of sediment discharge, together with the grain size composition of the suspended material, regional oceanographic conditions and local topographic features (Peukert et al. 2018; Gillard et al. 2019; Christiansen et al. 2020; Purkiani et al. 2021). Consequently, making accurate predictions of the dispersion of sediment particles and potential contaminants still remains one of the biggest challenges within deep-sea environmental risk and impact assessments (Peukert et al. 2018; Santos et al. 2018). Fundamental deep-sea research has evolved through the application of new monitoring techniques, but still remains difficult due to the extreme sampling conditions and associated high costs (Pape et al. 2017; Peukert et al. 2018; Lins et al. 2021). These efforts have led to a preliminary, rather than comprehensive, understanding of important ecological aspects such as drivers of meiofaunal distributions, specific life history traits, resilience and connectivity patterns, which hampers a correct assessment of faunal sensitivity to mining related pressures and the identification of thresholds (Gollner et al. 2017; Jones et al. 2017).

Improved knowledge on the tolerance levels and resilience of deep-sea ecosystems is necessary for the development of general indicators of change and management thresholds in light of mitigation actions (Foley et al. 2015; Levin et al. 2016; Clark et al. 2020; Smith et al. 2020; Hitchin et al. 2023). Benthic organisms that inhabit abyssal sediments are adapted to specific environmental conditions (e.g., low temperature, high pressure) with limited natural variability and therefore display slow growth and reproduction rates and specialized feeding strategies (Jones et al. 2017; Gollner et al. 2017; Santos et al. 2018). Moreover, due to the low natural sedimentation rates and low turbidity that characterize the abyss, there are major concerns about the impact of the sediment plume that will be created during mining and its possibly far-reaching dispersal (Aleynik et al. 2017; Peukert et al. 2018). The correct assessment of behavioral responses of biological communities to disturbance-related effects such as increased sedimentation, strongly depends on the ability to perform *in-situ* observations or controlled laboratory experiments. However, representative deep-sea tolerance studies of benthic species to sediment blanketing are scarce, due to the extreme sampling conditions, their restricted accessibility and concomitant limited ship time (Santos et al. 2018). Moreover, specialized sampling tools do exist to collect sediment and water samples that maintain *in-situ* conditions, but it is very difficult and costly to retrieve and transport them for further laboratory investigations (Santos et al. 2018; Mevenkamp et al. 2019). Hence, it

will be important to consider complementary approaches to support data acquisition for sediment load risk assessments (Santos et al. 2018; Hitchin et al. 2023).

During spring 2019, a small-scale seabed disturbance experiment was performed with a dredge (hereafter referred to as 'the dredge experiment') on board of the German research vessel SONNE in the German CCZ contract area in the frame of the MiningImpact2 project (Haeckel and Linke 2021). The dredge experiment served as a simulation of mining-related disturbances such as sediment removal and redeposition, which proved to be very valuable due to its extensive plume dispersal and ecosystem monitoring (Haeckel and Linke 2021). Within this study, responses of the soft-sediment benthic ecosystem component are investigated from samples taken for sediment characteristics (i.e., grain size, nutrients and pigments) and metazoan meiofaunal communities. The main objective was to investigate if this approach is suitable to detect short-term (< 1 month after disturbance) ecological responses to i) direct impacts (by comparison of the baseline *vs.* dredge track area) and ii) indirect impacts (comparing baseline *vs.* sediment plume areas). By using two techniques to study meiofaunal responses (i.e., morphological and metabarcoding analysis), we were also able to compare both methods and their results to determine the best methodology for future deep-sea meiofaunal monitoring studies. Additionally, we examined how benthic measurements can be combined with numerical modelling of sedimentation to enhance our knowledge of meiofaunal resilience to increased levels of sediment deposition. The integrated results are used to describe the lessons learned from this disturbance study.

Material and methods

Study area and sampling design

The Clarion-Clipperton Zone (5.1×10^6 km^2), is situated in the North-East Pacific Ocean and is characterized by high densities of polymetallic nodules (ISA 2011). The dredge experiment site was located within the eastern German contract area (Fig. 1) which showed limited topographic variability (4117–4125 m depth). The study site was also situated at sufficient distances from two other sampling sites (5 km northeast from a "Reference site" and 9 km south from a "Trial site") to avoid that these areas were affected by the experiment.

The dredge experiment consisted of 3 phases during which a wide array of oceanographic, biological, biogeochemical and geologic investigations were performed (Haeckel and Linke 2021). On 04/04/2019, the first "pre-impact" phase was initiated, during which Baseline samples were collected, together with the deployment of the sediment
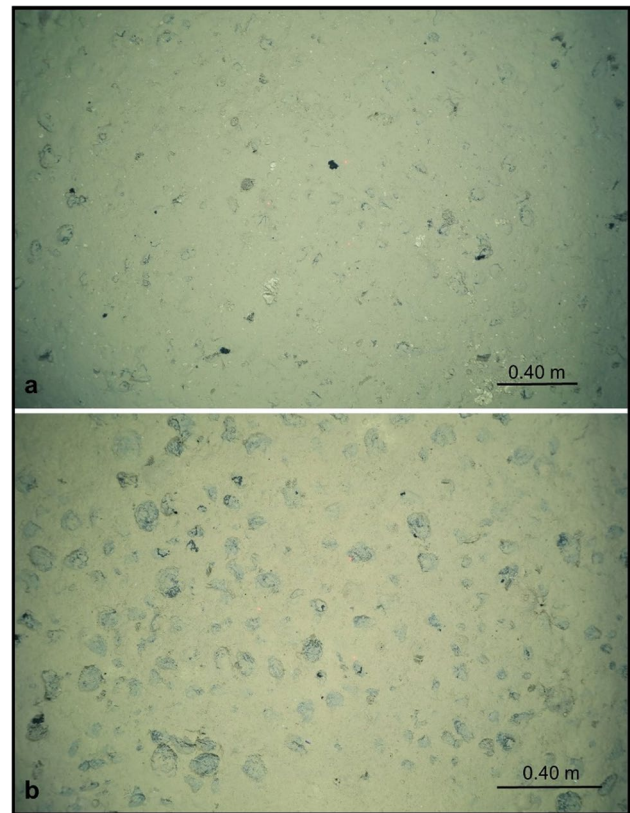

Fig. 1 Example photographs obtained by Ocean Floor Observation system (OFOS) surveys used to identify the different post-impact categories associated with increased sedimentation; **a** Thick cover and; **b** Thin cover

plume sensor array to monitor its dispersion. This monitoring array consisted of 15 platforms equipped with intercalibrated sensors to measure current velocities and particle concentrations (Haeckel and Linke 2021; Haalboom et al. 2022). These platforms were placed on the seafloor at three distances (100, 200, and 300 m) from the dredge tracks by means of a remotely operated vehicle (ROV Kiel 600) (Haeckel and Linke 2021; Haalboom et al. 2022). Additionally, 16 Sediment Level Indicator (SLIC) boxes were deployed throughout the sensor array, at closest distances of 50 m from the dredge tracks to collect resuspended sediment (Haeckel and Linke 2021; Haalboom et al. 2022).

Throughout the second phase ("disturbance"), a chain dredge (1.2 m wide and ~ 500 kg) was towed 11 times for 12 h on 11/04/2019 over an average distance of 500 m for each track perpendicular to the expected prevailing current direction at a towing speed of 0.2 – 0.5 m s^{-1} (Haeckel and Linke 2021; Purkiani et al. 2021). In order to provide an indication of the course of the dredge over the seafloor, an underwater acoustic positioning system (Posidonia transponder beacon) was also attached at about 500 m above the dredge (Haeckel and Linke 2021). Afterwards, "immediate"

(i.e., one week following the disturbance) samples were collected inside the Dredge track areas to assess short-term direct impacts. The third and final, "post-impact" phase in which indirect impacts associated with increased sedimentation were investigated, was initiated on 27/04/2022. Photographs of the SLIC boxes together with video observations using the Ocean Floor Observation System (OFOS) were used to assess the sediment deposition gradient within the adjacent areas of the dredge experiment. Approximately one month after disturbance, the final post-impact samples were collected within two proposed sedimentation impact categories. This categorization was established in a qualitative manner (i.e., video surveys and SLIC boxes photographs) where Thick cover samples corresponded to well covered nodules (approximately several millimetres, Fig. 1a), while Thin cover samples only showed very limited blanketing (approximately < 1 mm, Fig. 1b).

Soft-sediment sampling

Soft-sediment samples were obtained by means of a TV-guided multiple corer (MUC) to allow targeted sampling within the dredge tracks and areas of sediment deposition. A total of 11 MUC deployments (i.e., sampling stations), were performed within the proposed impact categories (Fig. 2) and per station, 1 to 2 MUC cores (inner diameter: 96 mm) were collected for meiofaunal samples (morphology and metabarcoding analysis) (Table 1). A total of six cores (morphological: n = 2, metabarcoding: n = 4) were taken prior to the dredge experiment (Baseline impact category), together with 10 cores (morphological: n = 4, metabarcoding: n = 6) within the Dredge track impact category,

one week post-dredge (Table 1). One month post-dredge, 16 cores were obtained in the sedimentation areas: Thick (morphological: n = 3, metabarcoding: n = 4) and Thin (morphological: n = 4, metabarcoding: n = 5) cover impact categories (Table 1). In addition, one core was collected for each deployment for environmental analysis, which were sliced vertically in intervals of 0–1, 1–5, and 5–10 cm, transferred to zip-lock bags and stored at -20 °C. For the cores collected for meiofaunal samples, the overlying water was removed and poured through a 32 μm sieve. Next, the top 0–5 cm sediment layer was sampled and transferred into a plastic container, together with the sieve residue. Samples for morphological studies were fixed with a 4% formaldehyde solution and stored at room temperature (RT). Samples for metabarcoding analysis were frozen at -80 °C on board and stored at -20 °C in the laboratory (Ghent University, UGent).

Analysis of environmental variables

Sediment grain size was determined by means of laser diffraction using the Malvern Mastersizer HYDRO 2000 and sediment fractions were classified according to (Wentworth 1922). Granulometric variables used within this study included median grain size (MGS) together with percentages of sand (> 63 μm), clay (< 4 μm) and silt (> 4 μm < 63 μm). Nutrient analysis of percent total organic carbon (TOC) and percent total nitrogen (TN) contents was performed with an Element Analyzer Flash 2000. Prior to analysis, sediment samples were homogenized and acidified with 1% HCl solution to remove any inorganic carbon compounds. In addition, the TOC and TN values were also used to calculate the C/N ratio for each sample. Pigment analysis for the acquisition

Fig. 2 Map of the dredge experiment site situated in the German license area. Black lines correspond to the dredge tracks and grey symbols represent the locations of the multicorer (MUC) samples obtained for meiofaunal analyses (morphological and metabarcoding samples) for the different impact categories (circles: Baseline, triangles: Dredge track, squares: Thick cover and pentagons: Thin cover)
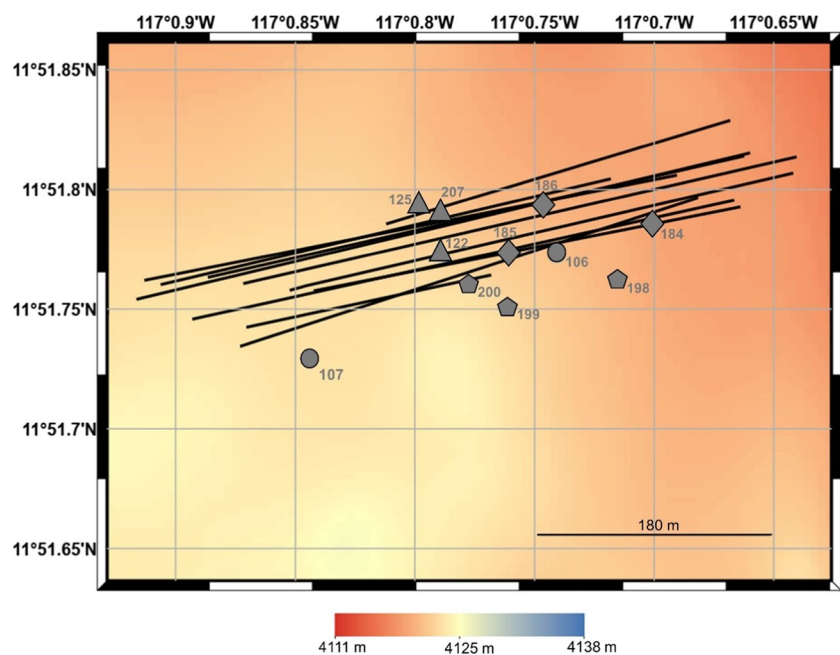
Table 1 Multicorer (MUC) samples collected for meiofaunal analyses. Samples are reported per station, MUC deployment and core label per analysis type, the date of sampling, geographical location (coordinates in degrees, minutes), water depth (m), together with their corresponding impact category (Baseline, Dredge track, Thick cover, Thin cover)

Station	MUC	Morphological (Core no.)	Metabarcoding (Core no.)	Date of sampling	Latitude (° N)	Longitude (° W)	Water depth (m)	Impact category
106	22	06	12/18	07/04/2019	11° 51.773′	117° 00.740′	4119	Baseline
107	23	18	16/17	07/04/2019	11° 51.729′	117° 00.844′	4121	Baseline
122	24	13	15/18	12/04/2019	11° 51.773'	117° 00.790'	4124	Dredge track
125	26	13/20	14/17	13/04/2019	11° 51.793'	117° 00.797'	4120	Dredge track
207	41	17	16/18	16/05/2019	11° 51.790′	117° 00.789′	4124	Dredge track
184	35	09	05/15	11/05/2019	11° 51.785′	117° 00.701′	4116	Thick cover
185	36	11	09/13	11/05/2019	11° 51.774′	117° 00.760′	4120	Thick cover
186	37	14	/	12/05/2019	11° 51.793′	117° 00.747′	4116	Thick cover
198	38	/	17	15/05/2019	11° 51.780'	117° 00.713'	4115	Thin cover
199	39	12/17	18/19	15/05/2019	11° 51.751′	117° 00.761′	4119	Thin cover
200	40	17/20	14/15	15/05/2019	11° 51.761′	117° 00.777′	4121	Thin cover

of Chlorophyll-a (Chl-a) concentrations was done according to Van Heukelem and Thomas (2001). After addition of 90% acetone, freeze-dried samples were sonicated and extracted overnight at 4 °C. After filtration, the extract was injected into an Agilent HPLC with fluorescence detector (type 1200 Infinity II, Agilent Technologies, Diegem, Belgium) equipped with an Eclipse XDB C8 column. The sum of Chl-a and phaeopigment concentrations was calculated and is further referred to as the Chloroplast Pigment Equivalent (CPE).

Meiofauna morphological analysis

The sediment cores collected for meiofaunal morphological analysis were rinsed with tap water over a 32 μm sieve, while the > 1 mm fraction residue was separated, fixed with 4% formaldehyde and stored at RT. Meiofauna was extracted from the remaining sediment according to Burgess (2001) by density-gradient centrifugation (3 × 12 min, at 1905 rcf) with the colloidal silica polymer Ludox HS-40 as flotation medium (density of 1.18 g/cm^3). The supernatant was poured over a 32 μm sieve and the residue was collected, fixed with 4% formaldehyde, stained with Rose Bengal and stored at RT. Afterwards, meiofaunal organisms were sorted, counted and identified at higher taxonomic level using a stereomicroscope. In addition, approximately 100 nematodes were hand-picked at random from each sample, transferred to anhydrous glycerol (De Grisse 1969) and mounted on slides. Nematoda identifications (genus level) were done at the Mixed Research Unit, UMR6197 Biologie et Ecologie des Ecosystèmes marins Profonds (University Brest, CNRS, Ifremer). Within our samples, two genera of the family Monhysteridae were found: *Monhystrella* and *Thalassomonhystera*. However, the identification of this family is characterized by a confusing taxonomic history (Fonseca and Decraemer 2008) and establishing morphological differences between these genera was sometimes challenging, especially due to the small body size of the nematodes. Furthermore, some authors have proposed a transfer in species between these two genera (Fonseca and Decraemer 2008). For these reasons, it was decided to remain at the family level for the Monhysteridae. Prior to statistical analysis, meiofauna counts were converted to abundances per surface area (i.e., ind. /10 cm^2).

Metabarcoding analysis

Library preparation Meiofauna was extracted from half of the frozen sediment into sterile Milli-Q water by density-gradient centrifugation (3 × 12 min, at 1905 rcf) with the colloidal silica polymer Ludox HS-40 as a flotation medium (specific density of 1.18 g/cm^3). The third and last residue was then centrifuged again for 10 min at 6350 rcf, and the supernatant removed. The pellet was resuspended and preserved in 500 μL of cetyltrimethylammonium bromide (CTAB) buffer at -20 °C and used for subsequent DNA extraction. Genomic DNA was extracted by adding 6 μL of proteinase-K [10 mg/mL] and centrifuged for 5 min at 14,000 rpm at room temperature. The pellet was ground, bead-beaten for 2 min at 30 cycles per second and incubated at 60 °C for 1 h. Ammonium acetate (250 μL, 7.5 M) was added and tubes were centrifuged for 10 min at 14,000 rpm at RT. The supernatant (750 μL) was transferred into a new sterile tube, 750 μL of cold 80% isopropanol solution was added, mixed, incubated for 30 min at RT, and centrifuged for 15 min at 14,000 rpm at 4 °C. The supernatant was

removed, 1 mL of washing buffer (76% EtOH and 10 mM ammonium acetate solution) was added, tubes were incubated for 30 min on ice to remove any salts and centrifuged for 5 min at 14,000 rpm at 4 °C. Finally, the supernatant was removed and 20 µL of sterilized water was added.

The 18S (V1-V2 region) ribosomal locus was amplified using the primers SSU_F_04-SSU/22_R (GCTTGTCTCAAAGATTAAGCC, TCCAAGGAAGGCAGCAGGC, respectively, (Blaxter et al. 1998)) which were constructed with Illumina overhang adapters as described in "16S Metagenomic Sequencing Library Preparation" (https://support.illumina.com/documents/documentation/chemistry_documentation/16s/16s-metagenomic-library-prep-guide-15044223-b.pdf). Each sample was amplified in triplicate with the following PCR conditions: 95 °C 2 min, 30x(95 °C 1 min, 57 °C 45 s, 72 °C 1 min), 72 °C 10 min. The mix consisted of 8.4 µL PCR-grade H_2O, 4 µL Phusion Buffer, 4 µL Dye, 0.4 µL dNTP [10 mM], 1 µL forward and reverse primer [10 µM], 0.2 µL Phusion Hot Start II High Fidelity Polymerase (New England BioLabs, U.S.A.) and 1 µL DNA template (diluted 1/10). In the event of failed amplification, DNA templates were diluted 1/50 in PCR-grade H_2O and/or 2 µL template were used. PCR products were run on a 1% agarose electrophoresis gel, triplicates were pooled, purified using Agencourt AMPure XP beads and run on Bioanalyzer 2100 High Sensitivity to confirm length and size distribution of the PCR fragments. Library indexing was completed using the FC131-1002 NexteraXT Index Kit (Illumina, U.S.A.) and Kapa High Fidelity PCR kit (Kapa Biosystems, U.S.A.). The mix consisted of 11.25 µL PCR-grade H_2O, 5 µL Buffer, 0.75 µL dNTP [10 mM], 2.5 µL Index1 and Index2, 0.5 µL Kapa Hot Start High Fidelity Polymerase and 2.5 µL PCR product. These were then purified using Agencourt AMPure XP beads and 11 randomly chosen samples were run on Bioanalyzer 2100 High Sensitivity to confirm successful indexing. DNA was quantified using Qubit® dsDNA High Sensitivity Assay Kit in all samples for pooling. Finally, the pooled library was sequenced at Macrogen on Illumina MiSeq-v3 2×300 bp paired-end read run.

Bioinformatic analyses Gene-specific adapters were removed from the 3' and 5' end of the reads using Cutadapt (v2.8) (Martin 2011) as non-internal adapters. Amplicon Sequence Variants (ASVs) were generated using the default DADA2 pipeline (Callahan et al. 2016) with truncation of forward and reverse reads at 250 and 200 bp, respectively. Taxonomic assignment of ASVs was completed using the ribosomal database projector (RDP) Naïve Bayesian Classifier (Wang et al. 2007) in two steps. First, a large eukaryotic reference database was used composed of sequences extracted from Silva (Silva release 123 for QIIME1, 99% OTUs) and UGent marine nematode Sanger sequences (n=18,991). All ASVs which received a Nematoda label at the phylum level were then extracted. Taxonomy was re-assigned to these ASVs with a marine nematode-specific reference database (n=971). This approach has been shown to deliver the highest number of taxonomic assignments (Macheriotou et al. 2019). Community composition was visualised using the R package ampvis2 (Andersen et al. 2018). Next, the dataset was converted into a phyloseq object for downstream analyses in R (McMurdie & Holmes 2013). Samples were rarefied to the lowest number of sequences (n=19,702) after which the number of observed ASVs were calculated.
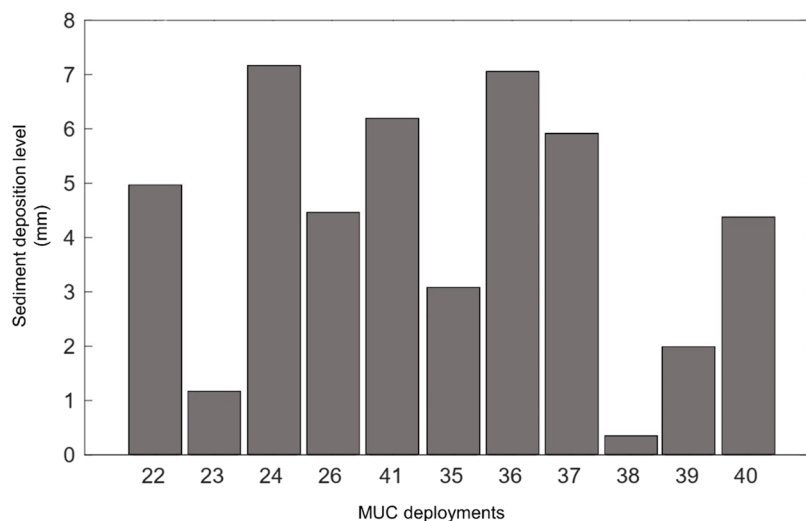
Statistical analysis

For the abiotic univariate variables (grain size, nutrients and pigments), a repeated measures two-way analysis of variance (ANOVA) test with factors "Impact category" (levels=="Baseline", "Dredge track", "Thick cover", "Thin cover") and " Sediment Depth" (levels=="0–1 cm", "1–5 cm", "5–10 cm") was used. For the biotic univariate variables obtained through the meiofaunal morphological analysis (total meiofaunal abundance and total nematode abundance) and metabarcoding analysis (number of ASVs), a one-way ANOVA (factor "Impact category") was performed to assess differences between impact categories. Prior to statistical analysis, data normality and homoscedasticity were assessed with a Shapiro and Levene's test, respectively. For the repeated measures two-way ANOVA, the assumption of sphericity was checked through the Mauchly's test and the Greenhouse–Geisser sphericity correction was applied for factors that violated this assumption. For the multivariate analyses, differences in terms of meiofaunal higher taxon (morphological analysis), nematode genus and Nematoda ASVs (obtained via morphological and metabarcoding analysis, respectively) composition between the different impact categories were investigated through a one-way permutational analysis of variance (PERMANOVA with factor "Impact category": levels=="Baseline", "Dredge track", "Thick cover", "Thin cover"), based on a Bray Curtis dissimilarity for the morphological datasets, while the UniFrac distance measure was applied for the metabarcoding dataset (Lozupone and Knight 2005). Meiofaunal higher taxon and nematode genus composition obtained through morphological analysis were first standardized to relative abundances to exclude differences in the number of specimens between samples. In addition, Permdisp tests were performed to assess the homogeneity of multivariate dispersions (distance to centroids). All analyses and graphs were completed using RStudio (v 1.2.5001, R v4.2.1), by means of the R packages plyr (Wickham 2011), car (Fox and Weisberg 2019), tidyverse (Wickham et al. 2019), vegan (Oksanen et al. 2019) and ggplot2 (Wickham 2009).

Numerical modelling of sediment redeposition patterns

A validated high-resolution sediment transport model (Purkiani et al. 2021) was used to study the linkage between meiofaunal samples and resulting data and simulated sediment re-deposition patterns. The ocean hydrodynamics were simulated using the Massachusetts Institute of Technology general circulation model (MITgcm) (Marshall et al. 1997; Adcroft et al. 2004). A sediment transport module was developed and coupled to the MITgcm, which was successfully applied to study the dynamics of sediment dispersion during the dredge experiment (Purkiani et al. 2021; Baeye et al. 2022). The model was forced on the open boundaries by hydrographic data obtained from the plume monitoring sensors as well as for the atmospheric parameters at the sea surface obtained by the European Centre for Medium-Range Weather Forecasts (ECMWF) reanalysis data. The horizontal model domain with a resolution of 21 by 25 m covered a region of 5×5 km^2 in which the dredge site was located, while the vertical resolution of the model varied from 1 m at the seafloor to 100 m at mid ocean depth. *In-situ* oceanographic and sediment parameters adopted from Gillard et al. (2019) were used to acquire sediment deposition levels. Assuming an initial sediment particle concentration of 35 mg/l in the plume under a low shear rate of ocean current field, the settling velocity of sediment particles was set to 25, 140, and 300 m/d for aggregates in what we refer to as class 1 (D25: 70 μm), class 2 (D50: 340 μm), and class 3 (D75: 590 μm), respectively. The sediment mass distribution was non-equally split so that class 1, class 2, and class 3 represent 25, 50, and 25% of total mass weight, respectively. Using a bulk density of freshly deposited sediments of 200 kg/m^3 and considering a porosity of 0.9 by volume for the newly deposited material, the sediment thickness levels for the accumulation of all three classes were calculated.

Additionally, positions of the MUC stations sampled for meiofaunal morphological analysis were interpolated on the model grid to assess their locations relative to the simulated sediment plume and to extract the sediment deposition height for each sample.

Results

Sediment deposition thickness simulations

Simulated sediment deposition levels (mm) were calculated for each MUC deployment for meiofaunal analysis and are visualized in Fig. 3. In general, it was found that each sample location was subjected to sedimentation ranging between < 1 mm to approximately 7 mm. The simulated sedimentation analysis showed that the highest sediment blanketing (6–7 mm) was observed within two Thick cover samples (MUC36/37), while the third sample of this impact category (MUC35) received approximately 3 mm of sediment. In addition, the majority of the samples from the Thin cover impact category received lower modelled sedimentation (< 3 mm), except MUC40 for which a sediment deposition thickness was calculated of 4.5 mm. Furthermore, this analysis revealed that during sample collection, a substantial level of sedimentation (4–7 mm) was also detected for all the samples collected within the Dredge track impact category.

Abiotic variables

Grain size analysis revealed that sediments in the 0–10 cm depth layer were mainly composed of silt ($66 \pm 8\%$), followed by sand ($20 \pm 10\%$) and clay ($14 \pm 2\%$). In general, average granulometric properties (MGS, percentages of sand, silt and clay) were comparable between impact categories and

Fig. 3 Bar plots of the simulated sediment deposition levels (mm) for the multicorer (MUC) samples taken for meiofaunal analyses (morphological and metabarcoding) during the dredge-experiment from each impact category: Baseline (MUC22/23), Dredge track (MUC24/26/41), Thick cover (MUC35/36/37) and Thin cover (MUC38/39/40)

sediment layers, except for the upper sediment layer (0–1 cm) of the Dredge track samples, which was characterized by higher average MGS and sand fraction and lower silt and clay fraction. However, this deviation could be attributed to the values found for one Dredge track sample (207_MUC41) and no statistical differences were found for all the granulometric variables (repeated measures two-way ANOVA, factors "Impact category" and "Sediment depth": $p > 0.05$). Detectable pigment concentrations (Chl-a, CPE) were only found within the upper sediment depth layers (0–1 cm, 1–5 cm), while the deeper layers (5–10 cm) showed values equal or close to zero (Fig. 4). This difference between sediment depth layers was confirmed through statistical analysis for Chl-a (repeated measures two-way ANOVA, factor "Sediment Depth": $p = 0.031$), while sediment depth differences for CPE were only significant at the 0.1 significance level (repeated measures two-way ANOVA, factor "Sediment Depth": $p = 0.052$). In terms of spatial differences between impact categories, trends indicated a slight decrease of average pigment concentrations within the 0–1 cm depth layer for the Dredge track samples, while highest average values were found for the Thin cover category, although differences were not statistically different (repeated measures two-way ANOVA, factor "Impact category": $p > 0.05$, Fig. 4).

TOC, TN and C/N values were comparable between sediment depth layers (repeated measures two-way ANOVA, factor "Sediment depth": $p > 0.05$). For the average TOC values, a decrease was observed within the upper sediment layer of Dredge track samples, whereas average TN values showed higher values for the two sediment redeposition categories (Thick and Thin cover) throughout the 0–10 cm depth

layers (Fig. 5) but no significant differences were found (repeated measure two-way ANOVA, factor "Impact category": $p > 0.05$). The C/N ratios were significantly different between impact categories (repeated measures two-way ANOVA, factor "Impact category": $p = 0.004$) and showed a clear reduction within the Dredge track, Thick cover and Thin cover compared to the baseline values (Fig. 6).

Meiofaunal responses: morphological analysis

Total meiofaunal abundance for each sample per impact category is presented in Fig. 7. Highest meiofaunal abundance was found for the Thin cover samples (179 ± 77 ind. /10 cm^2), followed by the Baseline samples (122 ± 83 ind. /10 cm^2) and Thick cover samples (116 ± 32 ind. /10 cm^2), while the Dredge track samples showed the lowest average abundances (112 ± 74 ind. /10 cm^2). However, meiofaunal abundances also showed considerable variability within impact categories and no statistically significant differences were observed (one-way ANOVA, factor "Impact category": $p > 0.05$). A total of 11 meiofaunal higher taxa (Amphipoda, Aplacophora, Copepoda, Gastropoda, Gastrotricha, Isopoda, Kinorhyncha, Nematoda, Ostracoda, Polychaeta and Tardigrada) and nauplius larvae were found. Meiofaunal composition was clearly dominated by the phylum Nematoda, which constituted > 96% of the total abundances, followed by Copepoda (3%) and nauplius larvae (1%) (Fig. 7). Whereas all three groups (Nematoda, Copepoda and nauplius larvae) showed higher relative abundances within the Thin cover samples compared to the other impact categories, no significant difference was detected in terms of meiofaunal higher
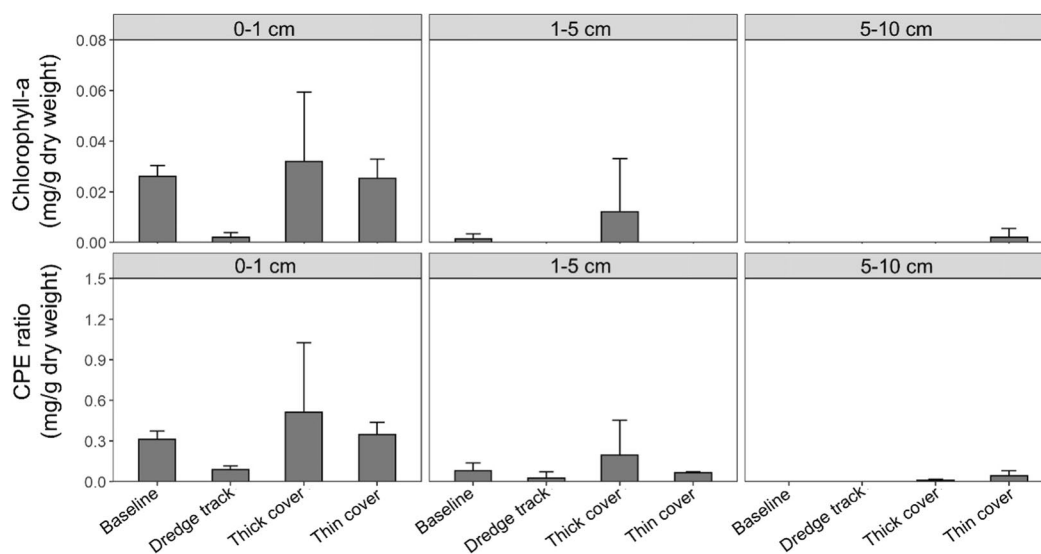

Fig. 4 Bar plots showing pigment concentrations: Chlorophyll-a (mg/g dry weight) and Chloroplastic Pigment Equivalents (CPE, mg/g dry weight) for each impact category (Baseline, Dredge track, Thick cover and Thin cover) per sediment depth layer (0–1, 1–5 and 5–10 cm). Error bars represent standard deviation
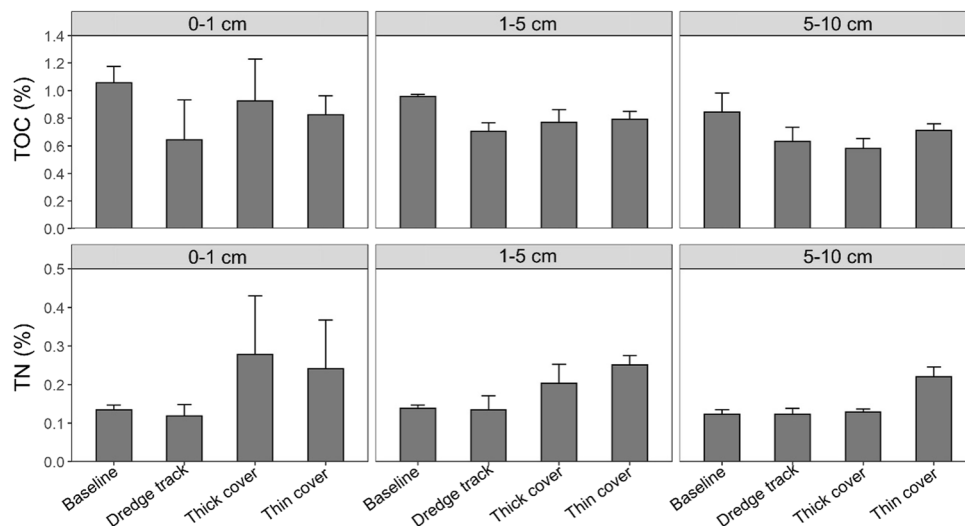
Fig. 5 Bar plots showing nutrient concentrations: Total organic carbon (TOC, %) and Total nitrogen (TN, %) for each impact category (Baseline, Dredge track, Thick cover and Thin cover) per sediment depth layer (0–1, 1–5 and 5–10 cm). Error bars represent standard deviation

taxon composition (one-way PERMANOVA, factor "Impact Category": $p > 0.05$, Permdisp test: $p > 0.05$).

Comparable to the meiofaunal abundance results, average nematode abundance was highest for the Thin cover samples (172 ± 75 ind. /10 cm^2), followed by the Baseline samples (116 ± 75 ind. /10 cm^2), Thick cover samples (111 ± 29 ind. /10 cm^2) and Dredge track samples (108 ± 73 ind. /10 cm^2), but these differences were not statistically significant (one-way ANOVA, factor "Impact Category": $p > 0.05$). Lower-taxonomical level Nematoda identifications based on morphology revealed a total of 68 genera from 25 families across all samples. The family Monhysteridae comprised 31% of the community and the genus *Acantholaimus* comprised another 13%. Remaining abundant genera, representing about 5% of the community were *Daptonema* and *Halalaimus,* followed by *Desmoscolex*

(4%), *Amphimonhystrella* (4%) and *Manganonema* (3%). Other genera contributed to a lesser extent to total nematode abundance and about 4% of the specimens was categorized as "undetermined" due to physical damage (e.g., broken, dried out, morphological features not clearly visible), making them unsuitable for further identification. Table 2 lists the most dominant taxa (relative abundance ≥ 2%) and revealed that specimens of Monhysteridae and *Acantholaimus* were shared across all impact categories as most abundant, while the relative contribution of other taxa showed considerable variation between impact categories (Table 2). However, results from the multivariate analysis did not reveal any statistically significant differences between impact categories in terms of nematode composition (one-way PERMANOVA, factor "Impact Category": $p > 0.05$, Permdisp test: $p = 0.005$).

Fig. 6 Bar plots for the calculated total organic carbon to nitrogen ratio (C/N ratio) for each impact category (Baseline, Dredge track, Thick cover and Thin cover) per sediment depth layer (0–1, 1–5 and 5–10 cm). Error bars represent standard deviation
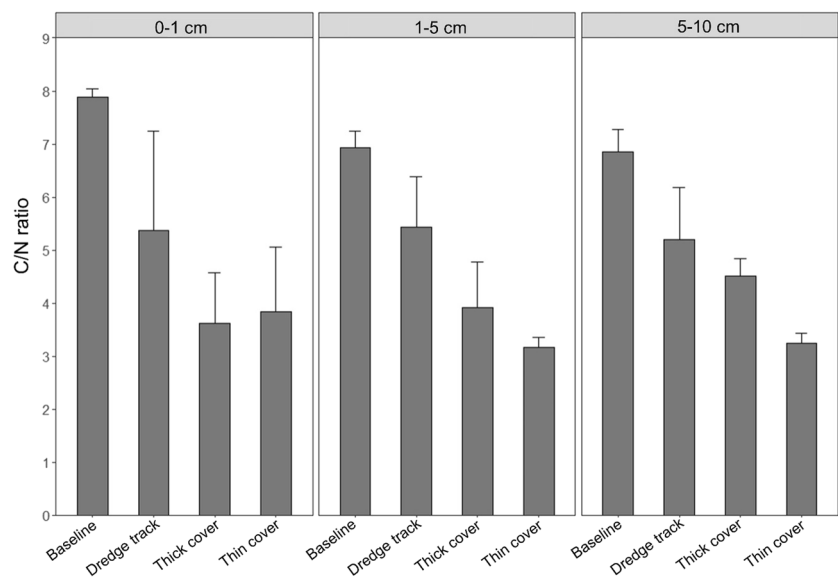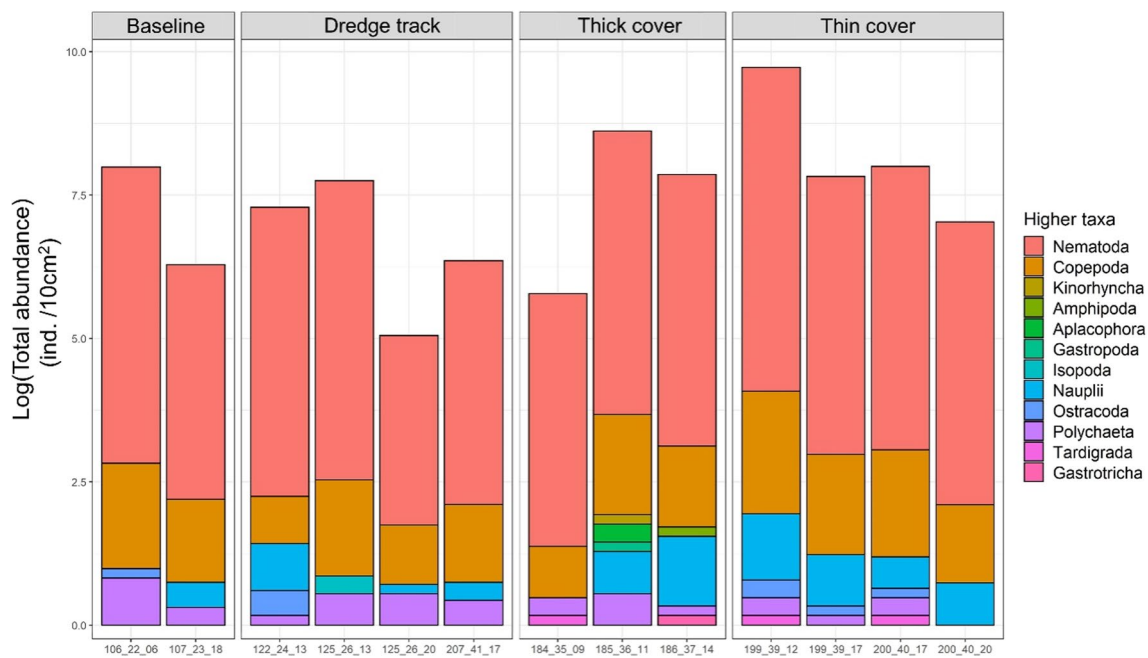
Fig. 7 Total meiofaunal abundance (ind. /10 cm^2) in the Baseline, Dredge track, Thick cover and Thin cover samples. Colour codes represent different higher taxa and nauplii (Crustacean larvae). Due to the dominance of Nematoda, values on the y-axis were re-scaled to log(1 + x) scale

Meiofaunal responses: metabarcoding

A total of 5,676,161 non-chimeric reads were generated from the 19 samples. The final rarefied dataset consisted of 2401 Nematoda ASVs. The highest number of ASVs was found in the Thin cover (244 ± 75), followed by Thick cover (196 ± 99), Dredge track (174 ± 117) and was lowest in the Baseline samples (155 ± 34) (Fig. 8). The most abundant genus across all samples was *Acantholaimus*, representing > 30% of the assemblage by read number. The remaining three most abundant genera, comprising > 5% of the community by read number, were *Halalaimus*, *Chromadorita* and *Desmoscolex* (Fig. 9). No statistically significant differences were detected between impact categories (one-way ANOVA, factor "Impact category": $p > 0.05$ and one-way PERMANOVA, factor "Impact Category": $p > 0.05$, Permdisp test: $p = 0.001$).

Table 2 Table of most dominant (relative abundance ≥ 2%) Nematoda genera for each impact category (Baseline, Dredge track, Thick cover and Thin cover)

Baseline samples		Dredge track samples		Thick cover samples		Thin cover samples	
Genus	%	*Genus*	%	*Genus*	%	*Genus*	%
Monhysteridae*	32	Monhysteridae*	29	Monhysteridae*	26	Monhysteridae*	41
Acantholaimus	14	*Acantholaimus*	13	*Acantholaimus*	14	*Acantholaimus*	12
Diplopeltoides	6	*Desmoscolex*	6	*Daptonema*	10	*Amphimonhystrella*	7
Halalaimus	6	*Halalaimus*	5	*Halalaimus*	6	*Diplopeltoides*	4
Manganonema	5	*Daptonema*	5	*Cobbia*	5	*Desmoscolex*	4
Marylynnia	4	*Aegialoalaimus*	3	*Amphimonhystrella*	4	*Halalaimus*	4
Desmoscolex	3	*Cobbia*	3	*Marylynnia*	4	*Manganonema*	3
Bolbolaimus	3	*Manganonema*	3	*Manganonema*	3	*Daptonema*	2
Molgolaimus	3	*Diplopeltoides*	3	*Desmoscolex*	2	*Chromadora*	2
Tricoma	3	*Bolbolaimus*	3	*Chromadora*	2	*Campylaimus*	2
Onchium	2	*Molgolaimus*	3	*Aegialoalaimus*	2	*Parastomonema*	2
Oxystomina	2	*Amphimonhystrella*	2	*Molgolaimus*	2	*Microlaimus*	2
		Scaptrella	2	*Diplopeltoides*	2	*Molgolaimus*	2
		Marylynnia	2	*Oxystomina*	2		

* Monhysteridae specimens were pooled to family level

Fig. 8 Number of Nematoda Amplicon Sequence Variants (ASVs) in the Baseline (circles), Dredge track (triangles), Thick cover (squares) and Thin cover (pentagons) samples. The crossbar and extent of the box represent the mean and standard deviation, respectively
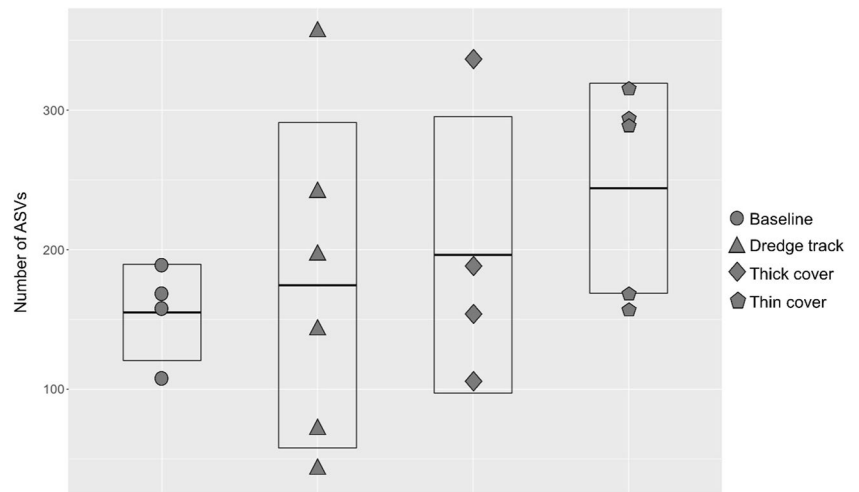

	Baseline	Dredge track	Thick cover	Thin cover
Acantholaimus	32.51	34.85	38.42	37.24
Halalaimus	19.84	21.33	10.21	25.24
Chromadorita	15.97	11.12	13.28	7.45
Desmoscolex	6.15	12.06	8.79	9.39
Phanodermopsis	7.79	8.17	1.66	4.11
Theristus	2.99	1.21	4.67	1.27
Subsphaerolaimus	2.79	1.26	1.29	3.91
Daptonema	2.2	2.92	1.94	1.71
Syringolaimus	1.26	4.52	0.22	0.43
Metoncholaimus	0	0	6.82	0
Bathylaimus	0	0	3.47	2.53
Oxystomina	2.88	0.08	1.03	0
Viscosia	0	0	2.81	0.5
Sphaerolaimus	1.52	0	0	1.32
Diplolaimelloides	0.18	0.47	0.88	0.53
Doliolaimus	0.48	0	0.81	0.68
Thalassoalaimus	0.71	0.03	0.02	0.85
Anticoma	0	0.09	0.59	0.78
Aegialoalaimus	0.06	0.4	0.49	0.21
Calomicrolaimus	0.27	0.1	0.67	0.14
Eumonhystera	0.52	0.13	0.47	0.06
Onchium	0	0.49	0	0.26
Leptolaimus	0.41	0.06	0.13	0.24
Ceramonema	0	0.33	0.37	0.02
Rhabdocoma	0.37	0.12	0.12	0.1
Desmolaimus	0.29	0	0.01	0.23
Deontolaimus	0.12	0.01	0.02	0.29
Bathyeurystomina	0	0	0.49	0
Linhystera	0.47	0	0	0
Molgolaimus	0	0	0.12	0.12
Diplopeltula	0	0.04	0.13	0.07
Remaining taxa (10)	0.21	0.21	0.07	0.32

Fig. 9 Relative read abundance (%) of genus-assigned Nematoda Amplicon Sequence Variants (ASVs) in the Baseline, Dredge track, Thick cover and Thin cover samples

Discussion

Meiofaunal responses to a small-scale seabed disturbance experiment

Merging meiofaunal measurements and numerical modelling

The combination of the sediment plume model analysis with measurements of the meiofaunal sampling resulted in

a detailed post-impact "simulated sediment deposition map", depicting the local modelled sediment redeposition patterns at the dredge site, superimposed with the MUC positions at the moment of sampling (Fig. 10). These analyses revealed that no modelled sediment plume dispersion was observed north of the dredge tracks, due to a dominant southward current (average speed of 4.4 cm/s), which was detected by the monitoring sensors during the experiment (Purkiani et al. 2021; Haalboom et al. 2022). As expected, sediment redeposition was highest and concentrated within the dredge

tracks, where the maximum modelled sediment thickness reached up to 9 mm (Fig. 10). At greater distances from the tracks, modelled sediment deposition levels decreased significantly, with 0.01 mm deposited 400 m of the impact centre (Fig. 10). Moreover, this analysis confirmed that the proposed impact categories and the MUC positions for meiofaunal sampling matched relatively well. Our study showed that the highest levels of modelled deposited sediment within the Dredge track and Thick cover areas did not result in significant differences in terms of meiofaunal abundances or ASV richness compared to the Baseline samples. In addition, samples from the Thin cover impact category that received lower levels of estimated sedimentation ($<$ 3 mm) were characterized by the highest average meiofaunal and Nematoda abundance and nematode diversity (ASVs), which may point to resuspension and dislocation of organisms from the directly impacted areas (Dredge track) to the surrounding sediments with limited sediment blanketing.

Meiofaunal resilience to sediment blanketing: a thinking exercise

Within this study, we explored the application of a combined methodology that incorporates expert-based insights from existing scientific literature, benthic measurements and numerical modelling to evaluate meiofaunal responses to different levels of modelled sedimentation. Performing such thinking exercises can lead to valuable information, which may ultimately contribute to the identification of suitable management thresholds (Santos et al. 2018;

Hitchin et al. 2023). Nematoda represent the most abundant group in abyssal sediments (Rex et al. 2006). They are very responsive to environmental conditions and have limited dispersal capacities, making them useful as bio-indicators to monitor human-induced disturbances and several shallow-water studies on their responses to sediment burial are available (Rosli et al. 2018). Additionally, deep-sea nematodes are also relatively well-studied in terms of their distribution patterns and diversity in the eastern CCZ (Miljutin et al. 2010; Vanreusel et al. 2010; 2016; Pape et al. 2017; Hauquier et al. 2019; Macheriotou et al. 2020; Pape et al. 2021). Therefore, this phylum was found useful to investigate the resilience of soft-sediment meiofauna to sediment blanketing.

Results in our study indicate that the highest simulated level of sediment burial (7 mm) did not seem to negatively affect nematode abundance and ASV richness. Furthermore, stations that received moderate levels of sediment deposition (3–5 mm) showed comparable values to the Baseline samples, while highest abundance was recorded for the Thin cover samples. These findings correspond with results from two previous studies that assessed the short-term effects (i.e., 11 to 16 days after disturbance) of different levels of sediment burial on meiobenthic organisms originating from mine tailings (inert iron ore, dead subsurface sediment) and crushed nodules (Mevenkamp et al. 2017, 2019). Both studies reported a strong upward vertical migration of meiofauna and a concomitant increased abundance in the measured deposited sediment layers (Mevenkamp et al. 2017, 2019), while adverse

Fig. 10 Sediment deposition map obtained through numerical modelling, depicting simulated sediment redeposition patterns (with different colours representing different levels of sediment deposition), superimposed with the multicorer (MUC) samples taken for meiofaunal morphological analyses (morphological and metabarcoding) within the different impact categories (circles: Baseline, triangles: Dredge track, squares: Thick cover and pentagons: Thin cover). The dark red contour line is set at 5 mm sediment deposition and spans an area of 17 m^2
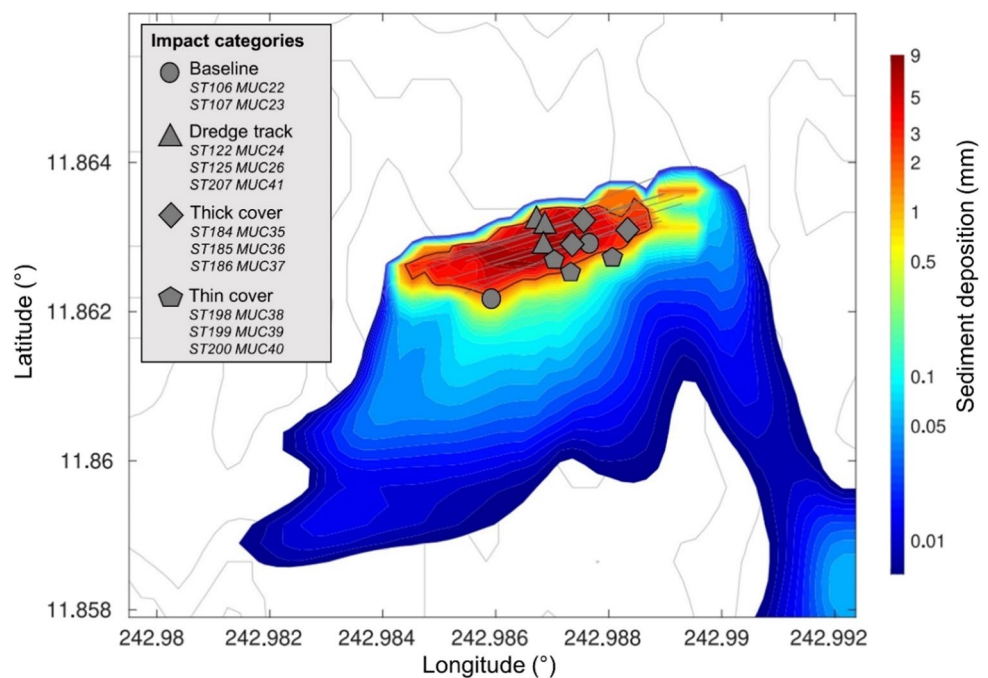
effects were only observed at measured sedimentation levels of 2 to 3 cm. Applying this to our findings, we suggest that the relatively low modelled sedimentation levels (< 1 cm) estimated within the dredge experiment did not have a short term negative effect (i.e., one month after disturbance) on Nematoda abundance or diversity (ASV richness). Moreover, the displacement of organisms from the resuspended sediments combined with the vertical migration of nematodes in the "receiving" sediments, might have led to increased abundances, especially in areas subject to limited sediment blanketing (< 3 mm).

However, it must be noted that the study by Mevenkamp et al. (2017) also revealed that for the mining tailings experiment, the upward migration was accompanied by higher nematode mortality for both substrate types (i.e., inert iron ore, dead subsurface sediment) and that impaired functioning such as organic matter mineralization was already detected for very limited induced sediment burial of about 0.1 cm (Mevenkamp et al. 2017). The latter is especially relevant considering that our results showed that Thin cover samples were characterized by higher nitrogen values and a significantly lower C/N ratio, implying that these sediments contain labile organic matter, which is more easily degradable for the inhabiting fauna (Arndt et al. 2013). As such, it remains uncertain whether the increased number of Nematoda that were found in the Thin cover samples represent living individuals, or dead specimens that were not yet decomposed one month after impact. Therefore, the aspect of "nematode viability" (i.e., discrimination between dead or living organisms) should be incorporated within impact studies to fully understand the resilience of meiofaunal communities subjected to sediment burial and potential implications on overall ecosystem functioning.

Morphological vs. metabarcoding analysis

Since meiofauna and certainly Nematoda constitute the majority of metazoan faunal densities and biomass within abyssal sediments, it is very important to define reliable methods for accurate taxonomic identifications of this group (Rex et al. 2006; Pape et al. 2017; Hauquier et al. 2019; Paulus 2021; Kürzel et al. 2022). However, for deep-sea systems, a large part of the meiofauna remains poorly characterized due to the lack of species-level descriptions and inadequate species identification keys to catalogue the vast amount of species (Paulus 2021; Kürzel et al. 2022). Processing samples for traditional morphological analyses is time-consuming and requires expert taxonomic knowledge attained through many years of experience (Le et al. 2022). While a morphological investigation of nematode communities can provide additional demographic information (e.g., size, sex, biomass) (Le et al. 2022), this analysis is typically only done for a subsample (100–150 individuals) owing to time constraints, leading to an underestimation of true biodiversity levels. On the other hand, DNA-based techniques such as metabarcoding analysis, assays the entire nematode assemblage and therefore represents a rapid method, better suited for small-bodied and rare/cryptic taxa (Macheriotou et al. 2019; Le et al. 2022). However, the effectiveness and taxonomic resolution are strongly dependent on the completeness and resolution of the used taxonomic reference databases, as well as the capacity of the genetic marker for species-level identification for the taxon under study (Macheriotou et al. 2019).

In this study, both methods yielded similar results as meiofaunal and nematode abundances (morphological analysis) together with ASV-based nematode richness (metabarcoding analysis), were highest within the Thin cover samples. Considerable within-group variability was evident in both datasets and no statistically significant differences were found between impact categories. Previous studies within the CCZ have revealed that deep-sea nematode assemblages are typically composed of a few abundant genera combined with a substantial amount of rare genera or so-called singletons (Miljutin et al. 2011; Pape et al. 2017; Hauquier et al. 2019; Pape et al. 2017). This trend was confirmed by our results as the majority of these dominant genera were identified by both techniques and corresponded to some of the most common deep-sea nematode genera such as *Acantholaimus* and *Halalaimus* (Miljutin et al. 2011; Pape et al. 2017, 2021; Hauquier et al. 2019). However, major differences were found for the Monhysteridae, which were the most abundant family for the morphological analysis but which were absent in the metabarcoding dataset. An absence of Monhysteridae sequences in molecular assessments of CCZ fauna has been documented before by Macheriotou et al. (2020) and the authors provided justifications for this observation. First is the bias introduced by the choice of the primer, which will inevitably amplify some taxa better than others. The presence of a DNA transition between the reverse primer sequence and that of the Monhysteridae reference may have reduced the DNA available for sequencing. Second, the high sequence similarity within the polyphyletic order Monhysterida, which includes the family Xyalidae and genera that were identified in the ASV data (e.g., *Daptonema*, *Theristus*, *Linhystera*), inhibits the ribosomal database projector (RDP) from assigning a taxonomic label at the chosen confidence level for taxa within Monhysteridae. We conclude that both methods can be used as complementary tools to study patterns of meiofaunal abundance and diversity. Nevertheless, certain problems related to metabarcoding (e.g., incomplete reference sequence databases, taxa-specific similarity) should be tackled to allow comparable compositional assessments.

Lessons learned and future considerations

The dredge experiment contained many useful elements in light of deep-sea mining studies, such as the extensive sediment plume monitoring which proved to be a suitable method to determine different impact categories and to apply an adaptive distance-based design to investigate effects within the areas with expected sediment resuspension (Haeckel and Linke 2021). Moreover, the wide array of measurements (i.e., biophysical, biogeochemical and biological samples) and visual mapping methods (i.e., high-resolution multibeam, photo/video transects) resulted in a substantial amount of valuable data for different ecosystem components. Despite these strengths, our findings were inconclusive without statistically significant meiofaunal responses, at least in terms of the variables studied herein. In the following section, potential reasons for the lack of detected effects are identified and elaborated upon, corresponding to some of the key issues raised by the deep-sea Environmental Impact Assessment (EIA) review paper by Clark et al. (2020). While these challenges are subdivided into three major categories namely, (1) natural variability of baseline conditions, (2) impact intensity and (3) sampling trade-offs, they are considered as strongly interrelated.

Natural spatial variability: dealing with uncertainty

To date, abyssal polymetallic nodule fields remain inadequately explored and available baseline information is insufficient (Clark et al. 2020; Amon et al. 2022). The ensuing scientific uncertainty complicates the incorporation of natural variability within deep-sea mining research, which is a requirement to study anthropogenic impacts in a robust manner (Hewitt et al. 2001). Examining benthic patterns and other abiotic characteristics such as nodule abundances and distributions also strongly depend on the considered spatial scale (Peukert et al. 2018). Due to their high diversity but relatively low abundances, meiofaunal communities in the deep sea, including the CCZ, exhibit considerable small-scale variability, so that even differences between cores from the same MUC deployments are often larger than those between samples from different deployments (Rosli et al. 2018; Uhlenkott et al. 2021). We therefore conclude that the observed variability, in combination with inadequate sampling (2 sampling stations, < 5 replicates/cores) for the Basleline impact category, did not allow for a reliable determination of baseline conditions in terms of meiofaunal abundance and community composition. More pre-impact sampling stations should be incorporated within future studies, that are distributed between the directly (i.e., inside the mining tracks) and indirectly impacted (i.e., in areas affected by the sediment discharge plume) areas. These stations must be extensively monitored in terms of environmental and biological properties which will minimize the effect of small-scale spatial heterogeneity (Methratta 2021).

Impact intensity: dealing with scale-dependency

Performing realistic, large-scale impact experiments is very challenging and most knowledge stems from small-scale disturbance trials (Jones et al. 2017; Clark et al. 2020). This has resulted in a mismatch between the likely nature (e.g., sediment reworking and sedimentation patterns) and extent (e.g., surface area covered, duration) of impacts that will occur during commercial mining (Jones et al. 2017; Clark et al. 2020). The dredge (1 m wide, 500 kg dry weight, Haeckel and Linke 2021) used in this study was undersized compared to the pre-prototype nodule collector vehicle Patania II, which is 4.5 m wide and weighs about 25 metric tons when submerged in water (https://deme-gsr.com/). In addition, the nature of impacts also likely differed as the dredging gear scraped the seafloor only superficially and irregularly, resulting in heterogenous patches of removed and accumulated sediments (Purkiani et al. 2021). This is probably not comparable to operating mining vehicles which are expected to remove and redeposit sediments to depths of up to several centimetres along extended stretches of the seabed (Peukert et al. 2018; Aleynik et al. 2017; Amon et al. 2022). Moreover, the indirect impacts created by the sediment plume were also small compared to the sediment blanketing that is expected to be induced by commercial mining operations, as the dredging mostly just pushed the sediments to the sides of the tracks with only limited sediment resuspension (Gillard et al. 2019; Purkiani et al. 2021). While the observed and simulated sediment depositions still exceed the natural sedimentation rates within these areas (Volz et al. 2018), near-field sedimentation resuspension is estimated to be up to several centimetres after commercial-scale nodule extraction (Gillard et al. 2019). From the above, it is evident that a second important reason for the lack of clear trends can be attributed to the unrepresentative impact intensity that was induced by the dredge used during this experiment.

Sampling trade-offs: dealing with multiple constraints

Monitoring and impact studies are often a compromise between the scientific objectives and financial and/or logistic constraints, especially when multiple scientific institutes are involved (Santos et al. 2018; Lins et al. 2021). This certainly applies to deep-sea research, where ship time is limited due to the remote working areas and financial costs are high because of the specialized technology that is needed (Santos et al. 2018; Lins et al. 2021). As a result, the trade-off between the number of sampling

stations versus the amount of deployments/samples taken for all the different variables will inevitable influence the statistical power (e.g., sensitivity to variability, effect size) of the study (Lins et al. 2021). The unbalanced and low number of meiofaunal samples in our study in combination with the high level of variability within impact categories and the small impact intensity of the dredge, were clearly insufficient to perform robust statistical analyses. A final but important aspect is that of inadequate temporal resolution within deep-sea research. Data from current studies are mostly based on one-point measurements with irregular periods in between successive sampling campaigns due to logistic and financial constraints (Lins et al. 2021; Amon et al. 2022). Extensive time-series data are needed to understand natural temporal variability (Clark et al. 2020; Lins et al. 2021; Amon et al. 2022), especially in abyssal ecosystems which are expected to show slow, delayed responses to disturbance (Miljutin et al. 2011; Gollner et al. 2017; Smith et al. 2020). The findings of our study can only reflect short-term (< 1 month) responses to simulated mining disturbance and should therefore be interpreted with caution. We conclude that deep-sea impact studies should be viewed as long-term projects with repeated, intensive sampling efforts (increased replication) at relevant time scales to verify the consistency of effects.

Declarations

Conflict of interest The authors declare no competing interests.

Ethics approval No approval of research ethics committees was required to perform this study.

Sampling and field studies All necessary permits for sampling and observation have been obtained by the authors from the competent authorities.

References

Adcroft A, Hill C, Campin JM, Marshall J, Heimbach P (2004) Overview of the formulation and numerics of the MIT GCM. Proceedings of the ECMWF Seminar Series on Numerical Methods, Recent Developments in Numerical Methods for Atmosphere and Ocean Modelling. Cambridge, Massachusetts, pp 139–149

Aleynik D, Inall ME, Dale A et al (2017) Impact of remotely generated eddies on plume dispersion at abyssal mining sites in the Pacific. Sci Rep 7:16959. https://doi.org/10.1038/s41598-017-16912-2

Amon DJ, Gollner S, Morato T et al (2022) Assessment of scientific gaps related to the effective environmental management of deep-seabed mining. Mar Policy 138:105006. https://doi.org/10.1016/j.marpol.2022.105006

Andersen KS, Kirkegaard RH, Karst SM, Albertsen M (2018) ampvis2: an R package to analyse and visualise 16S rRNA amplicon data. https://doi.org/10.1101/299537

Arndt S, Jørgensen BB, LaRowe DE, Middelburg JJ, Pancost RD, Regnier P (2013) Quantifying the degradation of organic matter in marine sediments: A review and synthesis. Earth Sci Rev 123:53–86. https://doi.org/10.1016/j.earscirev.2013.02.008

Baeye M, Purkiani K, de Stigter H et al (2022) Tidally driven dispersion of a deep-sea sediment plume originating from seafloor disturbance in the DISCOL area (SE-pacific ocean). Geosciences 12:8. https://doi.org/10.3390/geosciences12010008

Blaxter ML, De Ley P, Garey JR et al (1998) A molecular evolutionary framework for the phylum Nematoda. Nature 392(6671):71–75. https://doi.org/10.1038/32160

Boetius A, Haeckel M (2018) Mind the seafloor. Science 359:34–36. https://doi.org/10.1126/science.aap7301

Burgess R (2001) An improved protocol for separating meiofauna from sediments using colloidal silica sols. Mar Ecol Prog Ser 214:161–165. https://doi.org/10.3354/meps214161

Callahan BJ, McMurdie PJ, Rosen MJ et al (2016) DADA2: High-resolution sample inference from Illumina amplicon data. Nat Methods 13:581–583. https://doi.org/10.1038/nmeth.3869

Christiansen B, Denda A, Christiansen S (2020) Potential effects of deep seabed mining on pelagic and benthopelagic biota. Mar Policy 114:103442. https://doi.org/10.1016/j.marpol.2019.02.014

Clark MR, Durden JM, Christiansen S (2020) Environmental Impact Assessments for deep-sea mining: Can we improve their future effectiveness? Mar Policy 114:103363. https://doi.org/10.1016/j.marpol.2018.11.026

De Grisse AT (1969) Rediscription ou modifications de quelques techniques utilisées dans l'étude des nematodes phytoparasitaires. Mededelingen Rijksfaculteit der Landbouwwetenschappen, Gent 34:351–369

Durden JM, Lallier LE, Murphy K et al (2018) Environmental Impact Assessment process for deep-sea mining in 'the Area.' Mar Policy 87:194–202. https://doi.org/10.1016/j.marpol.2017.10.013

Foley MM, Martone RG, Fox MD et al (2015) Using ecological thresholds to inform resource management: Current options and future possibilities. Front Mar Sci 2:1–12. https://doi.org/10.3389/fmars.2015.00095

Fonseca G, Decraemer W (2008) State of the art of free-living marine Monhysteridae (Nematoda). J Mar Biol Assoc UK 88(7):1371–1390. https://doi.org/10.1017/S0025315408001719

Fox J, Weisberg S (2019) An R Companion to Applied Regression. https://socialsciences.mcmaster.ca/jfox/Books/Companion/index.html. Accessed 8 November 2022

Gillard B, Purkiani K, Chatzievangelou D et al (2019) Physical and hydrodynamic properties of deep sea mining-generated, abyssal sediment plumes in the Clarion Clipperton Fracture Zone (eastern-central Pacific). Element Sci Anthropo 7:5. https://doi.org/10.1525/elementa.343

Gollner S, Kaiser S, Menzel L et al (2017) Resilience of benthic deep-sea fauna to mining activities. Mar Environ Res 129:76–101. https://doi.org/10.1016/j.marenvres.2017.04.010

Haalboom S, Schoening T, Urban P et al (2022) Monitoring of Anthropogenic Sediment Plumes in the Clarion-Clipperton Zone, NE Equatorial Pacific Ocean. Front Mar Sci 9:882155. https://doi.org/10.3389/fmars.2022.882155

Haeckel M, Linke P (2021) RV SONNE Cruise Report SO268 - Assessing the Impacts of Nodule Mining on the Deep-sea Environment: NoduleMonitoring. GEOMAR Report 59. pp 802. https://doi.org/10.3289/GEOMAR_REP_NS_59_20

Hauquier F, Macheriotou L, Bezerra T et al (2019) Distribution of free-living marine nematodes in the clarion-clipperton zone: Implications for future deep-sea mining scenarios. Biogeosciences 16:3475–3489. https://doi.org/10.5194/bg-16-3475-2019

Hewitt JE, Thrush SE, Cummings VJ (2001) Assessing environmental impacts: Effects of spatial and temporal variability at likely impact scales. Ecol Appl 11:1502–1516. https://doi.org/10.2307/3060935

Hitchin B, Smith S, Kröger K et al (2023) Thresholds in deep-seabed mining: A primer for their development. Mar Policy 149:105505. https://doi.org/10.1016/j.marpol.2023.105505

International Seabed Authority (2011) Environmental Management Plan for the Clarion-Clipperton Zone. ISBA/17/LTC/7 International Seabed Authority, Kingston, Jamaica. https://www.isa.org.jm/documents/isba17ltc7

Jones DOB, Kaiser S, Sweetman AK et al (2017) Biological responses to disturbance from simulated deep-sea polymetallic nodule mining. PLoS One 12:e0171750. https://doi.org/10.1371/journal.pone.0171750

Kürzel K, Kaiser S, Lörz AN et al (2022) Correct Species Identification and Its Implications for Conservation Using Haploniscidae (Crustacea, Isopoda) in Icelandic Waters as a Proxy. Front Mar Sci 8:1–21. https://doi.org/10.3389/fmars.2021.795196

Le JT, Levin LA, Lejzerowicz F et al (2022) Scientific and budgetary trade-offs between morphological and molecular methods for deep-sea biodiversity assessment. Integr Environ Assess Manag 18:655–663. https://doi.org/10.1002/ieam.4466

Levin LA, Mengerink K, Gjerde KM et al (2016) Defining "serious harm" to the marine environment in the context of deep-seabed mining. Mar Policy 74:245–259. https://doi.org/10.1016/j.marpol.2016.09.032

Lins L, Zeppilli D, Menot L et al (2021) Toward a reliable assessment of potential ecological impacts of deep-sea polymetallic nodule mining on abyssal infauna. Limnol Oceanogr Methods 19:626–650. https://doi.org/10.1002/lom3.10448

Lozupone C, Knight R (2005) UniFrac: A new phylogenetic method for comparing microbial communities. Appl Environ Microbiol 71:8228–8235. https://doi.org/10.1128/AEM.71.12.8228-8235.2005

Macheriotou L, Guilini K, Bezerra TN et al (2019) Metabarcoding free-living marine nematodes using curated 18S and CO1 reference sequence databases for species-level taxonomic assignments. Ecol Evol 9:1211–1226. https://doi.org/10.1002/ece3.4814

Macheriotou L, Rigaux A, Derycke S, Vanreusel A (2020) Phylogenetic clustering and rarity imply risk of local species extinction in prospective deep-sea mining areas of the Clarion-Clipperton Fracture Zone. Proc R Soc B Biol Sci 287(1924):20192666. https://doi.org/10.1098/rspb.2019.2666

Marshall J, Adcroft A, Hill C, Perelman L, Heisey C (1997) A finite-volume, incompressible navier-stokes model for studies of the ocean on parallel computers. J Geophys Res 102:5753–5766. https://doi.org/10.1029/96JC02775

Martin M (2011) Cutadapt removes adapter sequences from high-throughput sequencing reads. EMBnet.Journal 17:10–12. https://doi.org/10.14806/ej.17.1.200

McMurdie PJ, Holmes S (2013) Phyloseq: An R Package for Reproducible Interactive Analysis and Graphics of Microbiome Census Data. PLoS One 8(4):e61217. https://doi.org/10.1371/journal.pone.0061217

Methratta ET (2021) Distance-Based Sampling Methods for Assessing the Ecological Effects of Offshore Wind Farms: Synthesis and Application to Fisheries Resource Studies. Front Mar Sci 8:1–18. https://doi.org/10.3389/fmars.2021.674594

Mevenkamp L, Guilini K, Boetius A et al (2019) Responses of an abyssal meiobenthic community to short-term burial with crushed nodule particles in the south-east Pacific. Biogeosciences 16:2329–2341. https://doi.org/10.5194/bg-16-2329-2019

Mevenkamp L, Stratmann T, Guilini K et al (2017) Impaired short-term functioning of a benthic community from a deep Norwegian fjord following deposition of mine tailings and sediments. Front Mar Sci 4:169. https://doi.org/10.3389/fmars.2017.00169

Miljutin D, Gad G, Miljutina MA et al (2010) The state of knowledge on deep-sea nematode taxonomy: how many valid species are known down there? Mar Biodivers 40(3):143–159. https://doi.org/10.1007/s12526-010-0041-4

Miljutin DM, Miljutina MA, Arbizu PM, Galéron J (2011) Deep-sea nematode assemblage has not recovered 26 years after experimental mining of polymetallic nodules (Clarion-Clipperton Fracture Zone, Tropical Eastern Pacific). Deep Res Part I Oceanogr Res Pap 58:885–897. https://doi.org/10.1016/j.dsr.2011.06.003

Miller KA, Thompson KF, Johnston P, Santillo D (2018) An overview of seabed mining including the current state of development, environmental impacts, and knowledge gaps. Front Mar Sci 4:418. https://doi.org/10.3389/fmars.2017.00418

Muñoz-Royo C, Peacock T, Alford MH et al (2021) Extent of impact of deep-sea nodule mining midwater plumes is influenced by sediment loading, turbulence and thresholds. Commun Earth Environ 2:1–16. https://doi.org/10.1038/s43247-021-00213-8

Oksanen J, Blanchet FG, Friendly M et al (2019) vegan: Community Ecology Package. R package version 2.5–6. https://CRAN.R-project.org/package=vegan

Pape E, Bezerra TN, Hauquier F, Vanreusel A (2017) Limited spatial and temporal variability in meiofauna and nematode communities at distant but environmentally similar sites in an area of interest for deep-sea mining. Front Mar Sci 4:1–16. https://doi.org/10.3389/fmars.2017.00205

Pape E, Bezerra TN, Gheerardyn H et al (2021) Potential impacts of polymetallic nodule removal on deep-sea meiofauna. Sci Rep 11:19996. https://doi.org/10.1038/s41598-021-99441-3

Paulus E (2021) Shedding Light on Deep-Sea Biodiversity—A Highly Vulnerable Habitat in the Face of Anthropogenic Change. Front Mar Sci 8:1–15. https://doi.org/10.3389/fmars.2021.667048

Peukert A, Schoening T, Alevizos E et al (2018) Understanding Mn-nodule distribution and evaluation of related deep-sea mining impacts using AUV-based hydroacoustic and optical data. Biogeosciences 15:2525–2549. https://doi.org/10.5194/bg-15-2525-2018

Purkiani K, Gillard B, Paul A et al (2021) Numerical Simulation of Deep-Sea Sediment Transport Induced by a Dredge Experiment in the Northeastern Pacific Ocean. Front Mar Sci 8:1–17. https://doi.org/10.3389/fmars.2021.719463

Rex MA, Etter RJ, Morris JS et al (2006) Global bathymetric patterns of standing stock and body size in the deep-sea benthos. Mar Ecol Prog Ser 317:1–8. https://doi.org/10.3354/meps317001

Rosli N, Leduc D, Rowden AA, Probert PK (2018) Review of recent trends in ecological studies of deep-sea meiofauna, with focus on patterns and processes at small to regional spatial scales. Mar Biodivers 48:13–34. https://doi.org/10.1007/s12526-017-0801-5

Santos MM, Jorge PAS, Coimbra J et al (2018) The last frontier: Coupling technological developments with scientific challenges to improve hazard assessment of deep-sea mining. Sci Total Environ 627:1505–1514. https://doi.org/10.1016/j.scitotenv.2018.01.221

Smith CR, Tunnicliffe V, Colaço A et al (2020) Deep-Sea Misconceptions Cause Underestimation of Seabed-Mining Impacts. Trends Ecol Evol 35:853–857. https://doi.org/10.1016/j.tree.2020.07.002

Thiel H, Schriever G, Ahnert A, Bluhm H, Borowski C, Vopel K (2001) The large-scale environmental impact experiment DISCOL—Reflection and foresight. Deep Sea Res Pt II 48:3869–3882. https://doi.org/10.1016/S0967-0645(01)00071-6

Tong SJW, Gan BQ, Tan KS (2022) Community structure of deep-sea benthic metazoan meiofauna in the polymetallic nodule fields in the eastern Clarion-Clipperton Fracture Zone, Pacific Ocean. Deep Res Part I Oceanogr Res Pap 188:103847. https://doi.org/10.1016/j.dsr.2022.103847

Uhlenkott K, Vink A, Kuhn T et al (2021) Meiofauna in a potential deep-sea mining area—influence of temporal and spatial variability on small-scale abundance models. Diversity 13:3. https://doi.org/10.3390/d13010003

Van Heukelem L, Thomas CS (2001) Computer-assisted high-performance liquid chromatography method development with applications to the isolation and analysis of phytoplankton pigments. J Chromatogr A 910:31–49. https://doi.org/10.1016/S0378-4347(00)00603-4

Vanreusel A, Fonseca G, Danovaro R et al (2010) The contribution of deep-sea macrohabitat heterogeneity to global nematode diversity. Mar Ecol 31:6–20. https://doi.org/10.1111/j.1439-0485.2009.00352.x

Vanreusel A, Hilario A, Ribeiro P et al (2016) Threatened by mining, polymetallic nodules are required to preserve abyssal epifauna. Sci Rep 6:26808. https://doi.org/10.1038/srep26808

Volz JB, Mogollón JM, Geibert W et al (2018) Natural spatial variability of depositional conditions, biogeochemical processes and element fluxes in sediments of the eastern Clarion-Clipperton Zone, Pacific Ocean. Deep-Sea Res Pt I 140:159–172. https://doi.org/10.1016/j.dsr.2018.08.006

Wang Q, Garrity GM, Tiedje JM, Cole JR (2007) Naïve Bayesian Classifier for Rapid Assignment of rRNA Sequences into the New Bacterial Taxonomy. Appl Environ Microbiol 73:5261–5267. https://doi.org/10.1128/AEM.00062-07

Washburn TW, Turner PJ, Durden JM et al (2019) Ecological risk assessment for deep-sea mining. Ocean Coast Manag 176:24–39. https://doi.org/10.1016/j.ocecoaman.2019.04.014

Weaver PPE, Aguzzi J, Boschen-Rose RE et al (2022) Assessing plume impacts caused by polymetallic nodule mining vehicles. Mar Policy 139:105011. https://doi.org/10.1016/j.marpol.2022.105011

Wentworth CK (1922) A Scale of Grade and Class Terms for Clastic Sediments. J Geol 30:377–392. https://doi.org/10.1086/622910

Wickham H (2011) The Split-Apply-Combine Strategy for Data Analysis. J Stat Softw 40(1):1–29. https://doi.org/10.18637/jss.v040.i01

Wickham H, Averick M, Bryan J et al (2019) Welcome to the tidyverse. Journal of Open Source Software 4(43):1686. https://doi.org/10.21105/joss.01686

Wickham H (2009) ggplot2: elegant Graphics for data analysis. Use R Springer, New York. https://doi.org/10.1007/978-0-387-98141-3_9